Inorganic Chemistry

Article

pubs.acs.org/IC

Cyclodextrin Capped Gold Nanoparticles as a Delivery Vehicle for a Prodrug of Cisplatin

Yi Shi, Jerry Goodisman, and James C. Dabrowiak*

Department of Chemistry, Syracuse University, 111 College Place, CST, Rm 1-014, Syracuse, New York 13244-4100, United States

Supporting Information

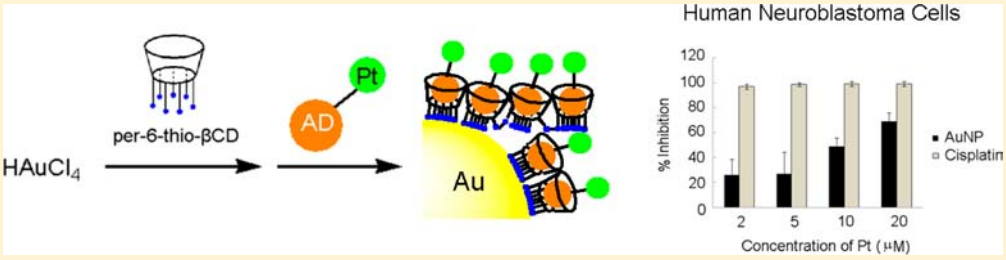

ABSTRACT: In this work, we explore the use of a quick coupling mechanism for "arming" a cyclodextrin coated gold nanoparticle (AuNP) delivery vehicle, **2**, with an adamantane-oxoplatin conjugate that is a prodrug of cisplatin, **3**, to produce a cytotoxic nanodrug, **4**. The two-part arming system, which utilizes the well-known guest−host interaction between β-cyclodextrin and adamantane, may be useful for rapidly constituting polyfunctional nanodrugs prior to their application in chemotherapy. The 4.7 ± 1.1 nm delivery vehicle, **2**, coated with per-6-thio-β-cyclodextrin (βSCD), was characterized using transmission electron microscopy and absorption spectroscopy, and the density of surface-attached βSCD molecules, ∼210 βSCD/AuNP, was determined using thermogravimetric analysis. Because ^{13}C NMR spectra of βSCD used in the study exhibited disulfide linkages and the observed surface density on the AuNP exceeded that possible for a close-packed mono layer, a fraction of the surface-attached βSCD molecules on the particle were oligomerized through disulfide linkages. Determination of the binding constant, K, for the **3**−βCD interaction using ^{1}H NMR chemical shifts was complicated by the self-association of **3** to form a dimer through its conjugated adamantane residue. With a dimerization constant of K_2 = 26.7 M^{-1}, the value of K for the **3**−βCD interaction (1:1 stoichiometry) is 400−800 M^{-1}, which is lower than the value, $K = 1.4 \times 10^3$ M^{-1}, measured for the **2**−**3** interaction using ICP-MS. Optical microscopy showed that when neuroblastoma SK-N-SH cells are treated with the nanodrug, **4** (**2**+**3**), clusters of gold nanoparticles are observed in the nuclear regions of living cells within 24 h after exposure, but, at later times when most cells are dying or dead, clustering is no longer observed. Treating the cells with **4** for 72 h gave percent inhibitions that are lower than that of cisplatin, suggesting that the Pt(IV) ions in **4** may be incompletely reduced to cytotoxic Pt(II) species in the cell.

INTRODUCTION

Gold nanoparticles (AuNP) exist in a wide range of sizes, shapes, and properties, and because their surface can be easily modified by attaching bioactive ligands such as drugs and proteins, they are being actively explored as new nanosized agents for treating cancer.[1−11] AuNPs having surface-attached recombinant tumor necrosis factor alpha and thiolated polyethylene glycol are currently in clinical trials in the United States for treating advanced stage cancer patients.[12] An attractive feature of AuNP is that they have the correct size to pass by passive diffusion through large holes in tumor vasculature where they become momentarily trapped. This effect, referred to as the enhanced permeability and retention effect (EPR), effectively increases the residence time of a toxic agent carried by the nanoparticle within the tumor mass, thus enhancing the effectiveness of the agent in arresting the cancer.

The platinum drugs, cisplatin carboplatin and oxaliplatin, by themselves or in combination with other agents, are in worldwide use for treating many forms of cancer.[7,13] The huge clinical success of these drugs has stimulated intense interest in incorporating them, or their biologically active components, into a variety of nanodelivery systems ranging from carbon nanotubes,[14] gold nanoparticles,[15−17] mesoporous silica,[18−21] dendrimers,[22−25] and liposomes and polymers.[26−28] While the platinum drugs can be readily conjugated to nanoparticles through their attached ligands, the fact that the nanoparticle itself often possesses targeting vectors and other agents that can directly react with Pt(II) or Pt(IV) suggests that the resulting polyfunctional assembly may not have sufficient long-term stability for formulation into a practical drug.[29] This concern is in stark contrast to the proven high stability of the platinum drugs, which in their ready to use infusion solutions have shelf-lives of 2−3 years.[30]

In an effort to explore, using a modular approach, ways in which a nanoparticle−platinum drug could be rapidly prepared prior to administration in chemotherapy, we studied the potential of the well-known guest−host interaction between

Received: April 21, 2013
Published: July 29, 2013

   dx.doi.org/10.1021/ic400989v | Inorg. Chem. 2013, 52, 9418−9426

Scheme 1. Synthesis of a βCD-Functionalized AuNP That Can Be Loaded via a Guest−Host Interaction with an Adamantane−Pt(IV) Complex

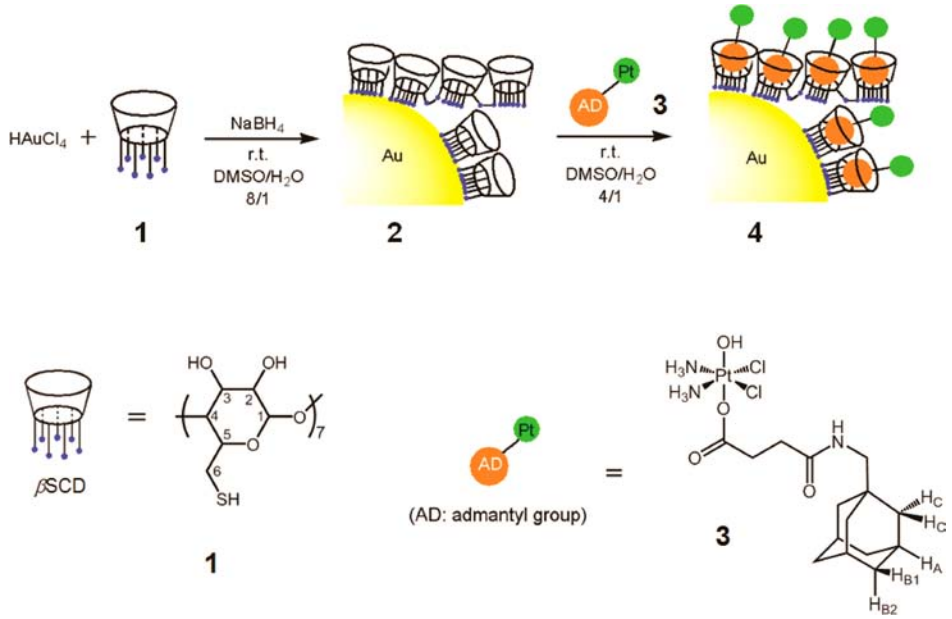

adamantane (AD) and β-cyclodextrin (βCD) to serve as a coupling mechanism for "arming" a gold nanoparticle with platinum drugs. Cyclodextrins, which bind small molecules through inclusion, enhance the solubility and activity of drugs,[31] facilitate immobilization of proteins on metallic surfaces,[32] control particle aggregation,[33] and when attached to AuNP produce vehicles capable of delivering drugs for therapeutic purposes.[34,35] Earlier, Prashar et al.[36] synthesized a unique analogue of carboplatin having a tethered AD group and showed that the inclusion complex of the analogue with βCD exhibits higher cytotoxicity toward neuroblastoma, SK-N-SH cells than carboplatin itself. Agarose gel electrophoretic studies with pBR322 DNA showed that the inclusion complex produced more platinum-DNA adducts than carboplatin itself, and, because fluorescein-labeled βCD localizes in the nucleus of the cell, the enhanced cytotoxicity of the inclusion complex may be due to cyclodextrin-enhanced delivery of platinum to nuclear DNA. In another study, Gibson and Brabec and their co-workers measured the cytotoxicity, mutagenicity, cellular uptake, and DNA and glutathione interaction of Pt(IV)−adamantane complex.[37] In another investigation, we tethered a 1-adamantanemethyamine group to the Pt(IV) anticancer agent, oxoplatin.[38] The latter conjugate formed a guest−host inclusion complex with βCD that was less toxic toward neuroblastoma SK-N-SH cells; reduction of the inclusion complex with the biological reducing agent ascorbic acid produced a Pt(II) product that bound to and unwound pBR322 form I DNA in a manner similar to that of cisplatin indicative of the formation of the 1,2 intrastrand cross-link.

In this Article, we use a modified procedure of Li et al.[39] to synthesize a 4.7 ± 1.1 nm gold nanoparticle capped with per-6-thio-β-cyclodextrin, βSCD, **1** (and a partially oligomerized product), and use the particle as a delivery vehicle for the earlier studied oxoplatin−AD conjugate that is a prodrug of cisplatin, Scheme 1. The thiol-cyclodextrin-capped AuNP was characterized using transmission electron microscopy (TEM) and absorption spectroscopy, and the amount of βSCD that was attached to the surface of the particle was determined using thermogravimetric analysis (TGA). In an effort to understand the nature of the interaction between the thiol-cyclodextrin-capped AuNP delivery vehicle and the oxoplatin−AD conjugate, the stoichiometry and binding constant of the interaction between βCD and the oxoplatin−AD conjugate were determined using ^{1}H NMR. We also measured the cytotoxicity of the oxoplatin-armed delivery vehicle toward neuroblastoma SK-N-SH cells and, with optical microscopy, found that the gold nanoparticles cluster within the nucleus of the cell.

EXPERIMENTAL SECTION

Instrumentation. UV−vis absorption spectra were recorded using a Cary 50 UV−vis spectrophotometer, with baseline correction in the region 200−800 nm in a 1 cm path length quartz cell. Mass spectra were obtained through positive electrospray ionization using a Bruker 12 T APEX- Qe FTICR-MS with an Apollo II ion source (COSMIC Lab, Norfolk, VA). Optical images of cells under white light illumination were obtained using a Leica DMI 4000 B microscope with a Leica DFC 340 FX digital firewire camera system (Syracuse Biomaterials Institute). Inductively coupled plasma mass spectrometry, ICP-MS data were obtained using a Perkin-Elmer Elan DRC-e instrument (SUNY College of Environmental Science and Forestry). One-dimensional ^{1}H NMR spectra and proton decoupled ^{13}C NMR data (75 MHz) were obtained using a Bruker Avance 300 MHz spectrometer at room temperature using a 5 mm probe. The proton resonance at 2.50 ppm, due to a small amount of the protonated form of DMSO in d_6-DMSO, was used as an internal chemical shift standard in the ^{1}H NMR studies, and the carbon resonance at 39.51 ppm was a chemical shift standard in the ^{13}C NMR studies.

Transmission Electron Miscroscopy (TEM). TEM measurements were performed using a JEOL 2000EX instrument operated at 120 kV with a tungsten filament (SUNY College of Environmental Science and Forestry, Syracuse, NY). The diameters of AuNP were determined using ImageJ software on populations >100 particles (counts) per determination.

Thermogravimetric Analysis (TGA). TGA was carried out on a TGAQ500 instrument using a heating rate of 5 °C/min. To determine the locations of weight changes, a series of trial runs prior to the final run were carried out. In step 1 of the heating profile, the βSCD-capped AuNP, **2**, was heated from room temperature to 100 °C where the

dx.doi.org/10.1021/ic400989v | Inorg. Chem. 2013, 52, 9418−9426

temperature remained for 30 min to eliminate water. In step 2 of the profile, the temperature was increased from 100 to 209 °C where the temperature was maintained for 1 h to eliminate DMSO from the sample. In step 3 of the profile, the temperature was increased from 209 to 800 °C to remove βSCD from the material.

Synthesis of Per-6-thio-β-cyclodextrin, βSCD, 1. The compound, per-6-iodo-β-cyclodextrin, required to synthesize **1** was made using the procedure of Defaye and Gadelle,[40] while **1** was synthesized using the method of Rojas et al.[41] As will be described below, **1** was found to be partially oxidized to oligomeric disulfides in the synthesis and/or workup of the product. Per-6-iodo-β-cyclodextrin: ^{1}H NMR (300 MHz, DMSO-d_6) δ = 3.24−3.47 (m, 21H), 3.56−3.68 (m, 14H), 3.80 (bd, 7H), 4.99 (d, 7H), 5.94 (d, 7H), 6.06 (d, 7H). Per-6-thiol-β-cyclodextrin, **1**: ^{1}H NMR (300 MHz, DMSO-d_6) δ = 2.16 (bd, ∼5.5H, SH), 2.73 (m, 7H, H-6a), 3.21 (bd, 7H, H-6b), 3.34 (m, 14H, H-2, H-4), 3.64 (bd, 14H, H-3, H-5), 4.95 (d, 7H, H-1), 5.83 (s, 7H, 3-OH), 5.92 (d, 7H, 2-OH). **1**: ^{13}C NMR (75 MHz, DMSO-d_6) δ = 26.0 (C-6, SH), 30.8, 35.8, 40.4 (C-6, CSSC), 72.0 (C-5), 72.3 (C-3), 72.6 (C-2), 85.0 (C-4), 102.2 (C-1). Mass spectrum of **1** (1:1 H_2O:MeOH with NaCl) expected m/z of $(C_{42}H_{70}O_{28}S_7)Na^+$ = 1269.2, observed m/z = 1269.2. See Supporting Information, Figures S2−4.

Synthesis of βSHCD-Capped AuNP, 2. The βSCD-capped AuNP **2** was prepared using a modification of the procedure of Liu et al.[39] Briefly, 48 mL of a DMSO solution containing 90 mg (2.34 mmol) of $NaBH_4$ and 24.0 mg (0.019 mmol) of **1** was added to 60 mL of a DMSO/H_2O 4/1 solution containing 12.2 mg (0.036 mmol) of $HAuCl_4$. The reaction solution was stirred at room temperature for 24 h after which time 96 mL of CH_3CN was added, which caused the formation of a precipitate that was collected by centrifugation. The precipitate was washed with 50 mL of a solution of mixed solvents CH_3CN and DMSO (1:1 v/v), was isolated by centrifugation, and washed a second time with 50 mL of ethanol. The material was isolated by centrifugation and dried in vacuo. The dried solid was taken up in 0.2 mL of H_2O, and the solution was kept at room temperature for 30 min before adding 0.6 mL of CH_3CN, which induced precipitation of purified **2**. The βSCD-capped AuNP was collected by centrifugation and dried in vacuo overnight to obtain 10.7 mg of dried product.

Formation of the Inclusion Complex, 4. Compound **3** was synthesized by the reaction of 1-adamantanemetylamine and the Pt(IV)−succinic acid complex in the presence of a coupling agent in DMSO.[38] To a solution of 0.75 mg of **3**, 1.29 μmol, dissolved in 0.4 mL of DMSO, was added a solution of 6.5 mg of **2**, 1.29 μmol of gold-attached βSCD, dissolved in 0.1 mL of H_2O. The reaction mixture was stirred overnight at room temperature, following which 1.5 mL of CH_3CN was added to induce precipitation of **4**, which was collected by centrifugation. The precipitate was washed with 2 mL of CH_3CN and DMSO (3:1 v/v), washed a second time with 1 mL of ethanol, and the drug-loaded vehicle (4.0 mg) was isolated by centrifugation and dried overnight in vacuo. The weight percentage of Pt in **4**, obtained through ICP-MS analysis, was 2.50%.

^{1}H NMR Studies of the Binding of 3 to βCD and the Self-Association of 3 in Solution. For studying the binding of the oxoplatin−AD conjugate **3** to β-cyclodextrin, βCD, a series of ^{1}H NMR spectra for various values of r, where r = [βCD]/[**3**], were collected in the solvent d_6-DMSO/D_2O 80/20, and plots of the chemical shift of protons on the adamantane group versus r were constructed. Compound **3** was initially dissolved in 480 μL of d_6-DMSO followed by the addition 120 μL of D_2O to give a final concentration of **3** of 16.7 mM. Weighed amounts of solid βCD were added to the solution containing **3** to give final values of r of 0.20, 0.41, 0.61, 0.82, 1.02, 1.52, 2.02, and 4.03. After we waited 2 h to ensure that equilibrium was reached, ^{1}H NMR spectra of the solutions were obtained.

^{1}H NMR spectra of **3** by itself in d_6-DMSO/D_2O 4:1 exhibited proton resonances for the adamantane group that were strongly dependent on the total concentration of **3** in solution. Because this indicated that the compound self-associates, this association was studied using ^{1}H NMR by diluting a 40 mM stock solution of the compound with the NMR solvent and recording spectra of the diluted solutions. Because similar concentration-dependent proton NMR spectra were also obtained for 1-adamantanemethylamine and 1-adamantanemethylalcohol, the self-association of **3** appears to involve the adamantane group and not the oxoplatin moiety; see Figures S5 and S6 in the Supporting Information.

Cell Cytotoxicity Studies. The studies involving human neuroblastoma (SK-N-SH) cells were carried out under standard conditions in a humidified, 37 °C, 5% CO_2 atmosphere in an incubator. The culture medium used for SK-N-SH cells was Eagle's minimum essential medium (EMEM) to which had been added 10% Fetal Calf Serum (FCS), 100 μg/mL streptomycin, 100 IU/mL penicillin, and 2.0 mM L-glutamine. Four solutions having Pt concentrations 2, 5, 10, and 20 μM were prepared by dissolving a weighed amount of **4** or cisplatin in the culture medium. To each of 60 wells, 6 groups of 10 wells each, in the central portions of four 96-well microplates were added medium alone containing no cells, group 1, and medium containing 5 × 10^4 cells/mL, groups 2−6. The cells were allowed to grow for 24 h, reaching ∼30% confluency, after which the medium was removed and replaced with 100 μL of medium containing compound having concentrations of 0, 2, 5, 10, and 20 μM Pt for groups 2−6, respectively. After 72 h exposure time, the medium in the wells containing cells was removed and replaced and washed twice with fresh medium. The number of live cells was determined using the CCK-8 assay (Dojindo Molecular Technologies, Inc., Rockville, MD) according to the supplier's protocol.

The percent inhibition of cell growth was calculated using eq 1, where I is the percent inhibition, A_T is the absorbance of wells with cells containing culture medium + Pt complex, A_C is the absorbance of wells with cells and culture medium, and A_M is the absorbance of wells without cells but with culture medium.

$$I = 100 \times \left[\frac{A_C - A_T}{A_C - A_M}\right] \quad (1)$$

RESULTS AND DISCUSSION

Gold nanoparticles, **2**, Scheme 1, were synthesized through a one-step reaction by reducing $HAuCl_4$ using $NaBH_4$ in the presence of per-6-thio-β-cyclodextrin, βSCD, **1**, in DMSO/H_2O. As is shown in Figure 1, **2** exhibits a surface plasmon peak

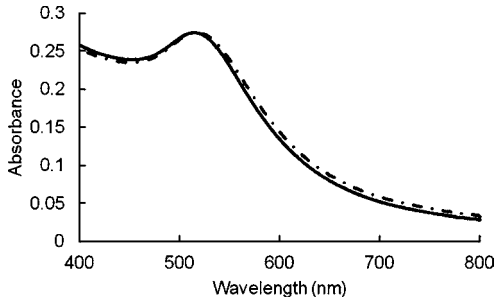

Figure 1. UV−vis absorption spectra of the βSCD capped AuNP, **2** (−), and the "armed" nanoparticle, **4** (**2**+**3**) (− · − · −), in aqueous solution.

at λ_{spr} = 515 nm, the position of which is consistent with the measured TEM diameter 4.7 ± 1.1, Figure 2.[42] Figure 1 shows that binding of **3** to **2** to produce the armed delivery vehicle **4** does not affect the position of the surface plasmon resonance of the nanoparticle, λ_{spr} = 515 nm, and Figure 2 indicates that the diameter of **4**, measured by TEM (D = 4.9 ± 1.0 nm), is the same or only slightly increased relative to that of **2**.

An important property of the cyclodextrin-capped AuNP, **2**, is the number of the oxoplatin−adamantane conjugates, **3**, that can be bound to the nanoparticle, which is related to the average number of bound cyclodextrin molecules per nano-

dx.doi.org/10.1021/ic400989v | Inorg. Chem. 2013, 52, 9418−9426

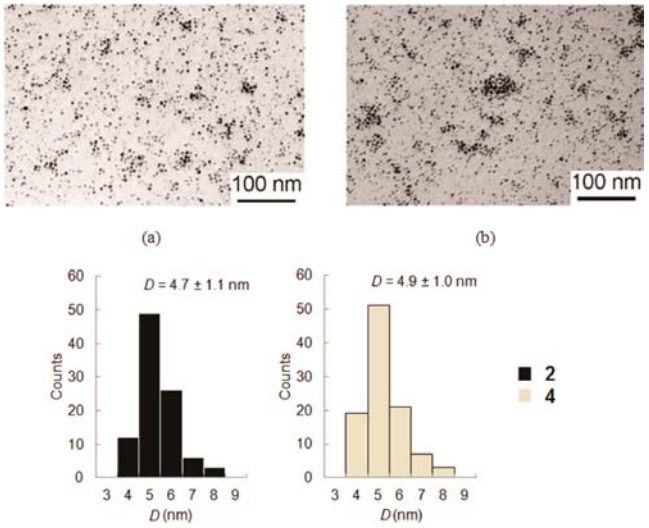

Figure 2. TEM images and diameter histograms of (a,c) **2** and (b,d) **4**.

particle. The amount of βSCD bound to the surface of the gold nanoparticle was determined using thermogravimetric analysis (TGA). From the data shown in Figure 3, the loss of weight

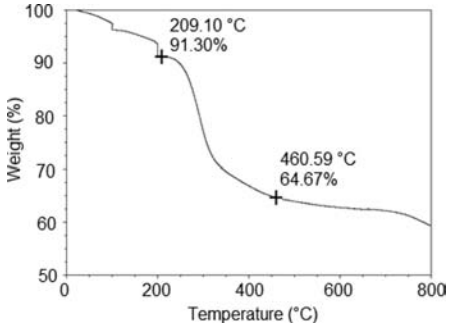

Figure 3. TGA curve of **2**. Following the loss of water and DMSO (100−91.30%), the decrease in weight of the particle due to loss of βSCD is 91.30% − 64.67% = 26.63%. The weight % values, determined by placement of the cursor on the TGA curve, are considered approximate values.

from **2**, attributed to the loss of βSCD from the sample, that is, the weight loss in the temperature range, 209−460 °C, is 26.63%. Although the weight of the sample decreases slowly for $T > 460$ °C, the weight of the sample remaining at this point, 64.67%, is considered the weight of gold in **2**.

The data from these measurements were entered into eqs 2 and 3,[43] where N is the average number of gold atoms per AuNP, ρ is the density for fcc gold (19.3 g/cm^3), D is the average core diameter of the particles (nm), M is the atomic weight of gold (197 g/mol), N_A is Avogadro's constant, and M' is the molecular weight of **1**, in this case considered as the thiolate form, 1240 g/mol.

$$N = \frac{\pi\rho}{6}\frac{(D/10^7)^3}{(M/N_A)} = 30.90D^3 \quad (2)$$

$$n = \frac{NM}{M'}\frac{\text{wt\%}(\mathbf{1})}{\text{wt\%(Au)}} = 4.91D^3\frac{\text{wt\%}(\mathbf{1})}{\text{wt\%(Au)}} \quad (3)$$

From the TEM (Figure 2), D = 4.7 nm, so that the calculated value of n, the number of βSCD molecules attached to the nanoparticle, is ∼210.

As a check on how much βSCD could be bound per nanoparticle, we considered the packing problem involving the surface area of a nanoparticle and surface-bound circles representing the βSCD molecules. The number of βSCD molecules that could occupy the surface of a nanoparticle in a close-packed monolayer array was calculated using eq 4, in which S_{Au} is the surface area of AuNP (nm^2), and S_1 is the surface area (nm^2) of the wider opening of βSCD, D = 1.54 nm.[44]

$$\frac{S_{Au}}{S_1} = \frac{2\pi D^2}{\sqrt{3}D^2} = 3.62\left(\frac{D}{d}\right)^2 \quad (4)$$

Using the experimental values in eq 4, the calculated coverage of the AuNP is ∼34 βSCD molecules per nanoparticle. This is much lower than the value found from TEM/TGA measurements, ∼210 βSCD molecules per nanoparticle.

To explain the difference between the observed and calculated coverage values, closer consideration was given to the structure of the βSCD ligand, the synthesis of which was initially reported by Rojas et al.,[41] and which was later attached to AuNP by Liu and co-workers.[39] Although the ^{1}H and ^{13}C NMR data for **1** generally agreed with those reported by Rojas et al.,[41] the number of thiol protons for the ligand in ^{1}H NMR spectra was somewhat lower than expected (observed ∼5.5H, calculated 7H), and, most importantly, the ^{13}C NMR spectrum of the compound exhibited four carbon resonances for C-6 of **1** (Scheme) when only one resonance for this carbon atom is expected. The ^{13}C NMR resonance at 26.0 ppm for βSCD is due to the expected thiol at C-6, but the three additional resonances at 30.8, 35.8, and 40.4 ppm are consistent with the compound having disulfide linkages at C-6.[45,46] This clearly shows that some of the thiol groups of **1** have been oxidized to disulfides during the synthesis and workup of the compound (Experimental Section, Figures S2, S3). Because both intra- and intermolecular disulfides with **1** are possible, some of the βSCD used in the synthesis of **2** was likely oligomerized through intermolecular disulfide bonds (Scheme 1); this explains the higher-than-expected coverage density of **1** on the surface of the nanoparticle. Despite attempts to detect oligomeric species in the mass spectrum of βSCD, only the molecular ion for sodiated monomeric **1** was observed (Figure S4).

In an effort to determine the binding stoichiometry and binding constant of **3** toward β-cyclodextrin, which is important for determining the ability of **2** to act as a delivery vehicle for **3**, ^{1}H NMR spectra of mixtures of **3** and β-cyclodextrin (βCD) were recorded. Figure 4 shows the NMR spectrum of a mixture containing the platinum-adamantane conjugate **3** (16.7 mM) and βCD (3.34 mM) in d_6-DMSO/D_2O 4:1, while Figure 5 shows the chemical shifts of protons H_A, H_B, and H_C (see Scheme 1 for assignments) on the substituted adamantane of **3** as functions of r, where $r = [\beta CD]/[\mathbf{3}]$, with [**3**] = 16.7 mM. As is evident from Figure 5, the chemical shifts of the adamantane protons on **3** increase with increasing r, indicating that these protons are deshielded in the host−guest complex that forms between the adamantane residue of **3** and β-cyclodextrin.

The chemical shift of each of the three protons on **3** is a weighted mean of the shifts when **3** is bound to βCD and when **3** is free: $\delta = f_b\delta_b + (1 - f_b)\delta_0$ where δ_b is the chemical shift when $[\beta CD]_0$ is very large and all of **3** is bound, and δ_0 is the

dx.doi.org/10.1021/ic400989v | Inorg. Chem. 2013, 52, 9418−9426

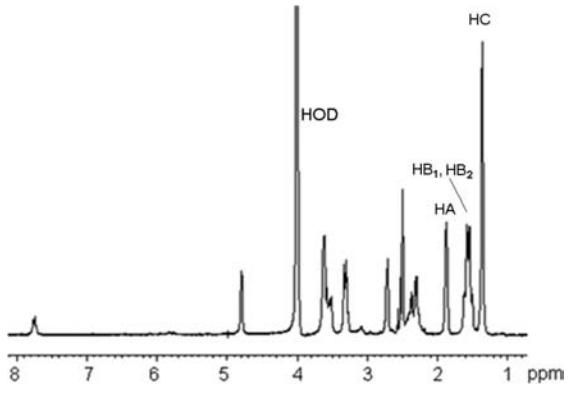

Figure 4. ^{1}H NMR of **3** (16.7 mM) and βCD (3.34 mM) in d_6-DMSO/D_2O 4:1 (v/v). See Scheme 1 for chemical shift assignments of the adamantane group.

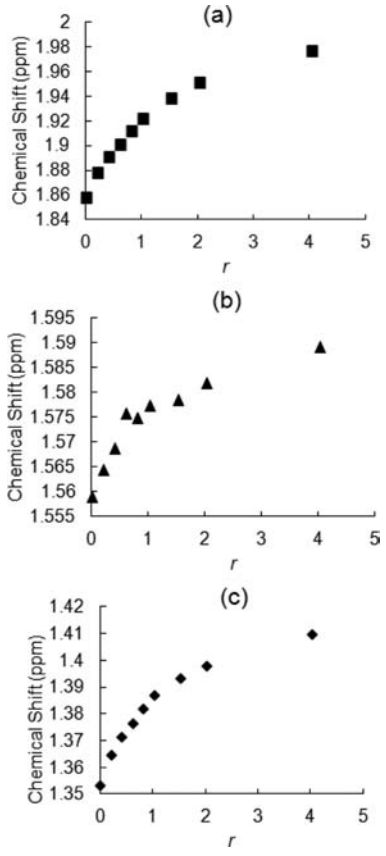

Figure 5. ^{1}H NMR chemical shifts of the adamantane protons of **3** in the presence of βCD versus r, where $r = [\beta\text{CD}]/[\mathbf{3}]$ with $[\mathbf{3}] = 16.7$ mM. For protons on (a) H_A, (b) H_B, and (c) H_C of the adamantane group, see Scheme 1.

chemical shift when $[\beta\text{CD}]_0$ is zero and all of **3** is unbound. It follows that

$$f_b = \frac{\delta - \delta_0}{\delta_b - \delta_0}$$

The fraction bound, f_b, is determined by the simple binding equilibrium:

$$\beta\text{CD} + \mathbf{3} \overset{K}{\rightleftharpoons} \beta\text{CD}{-}\mathbf{3} \qquad (5)$$

where K is the equilibrium constant for binding. In terms of f_b, we have

$$K = \frac{[\beta\text{CD}{-}\mathbf{3}]}{[\beta\text{CD}][\mathbf{3}]} = \frac{f_b[\mathbf{3}]_0}{\{[\beta\text{CD}]_0 - f_b[\mathbf{3}]_0\}\{(1 - f_b)[\mathbf{3}]_0\}} \qquad (6)$$

We determined K by fitting the NMR chemical shifts to this binding model.

There are two unknown parameters for each of the protons H_A, H_B, and H_C: δ_0 and δ_∞. With K, there are thus seven parameters to be determined. We found the values of the parameters that minimized the sum of the square deviations between calculated and measured shifts (27 data points in all). Details are found in the Supporting Information. The resulting value of K is 436 M^{-1}, with a large uncertainty. As shown in the Supporting Information, the last data points ($r = 4.02$) show by far the largest deviations, and the values of the parameters are very sensitive to errors in these points. If these are not used in the minimization, we obtain K = 813 M^{-1} showing that the value of K obtained can be correct only to an order of magnitude.

In the course of investigating the interaction of **3** with βCD, it was found that the NMR spectrum of **3** is itself dependent on the total concentration of the compound in solution, with the chemical shifts of the adamantane protons of **3** shifting to higher field when the concentration of the compound increases. This can be clearly seen in the spectra in Figure 6, where $[\mathbf{3}]$ = 2 and 40 mM, and the plots in Figure 7, which show the dependence of the chemical shifts of the adamantane protons on $[\mathbf{3}]$.

This indicated that **3** by itself associates in solution, according to

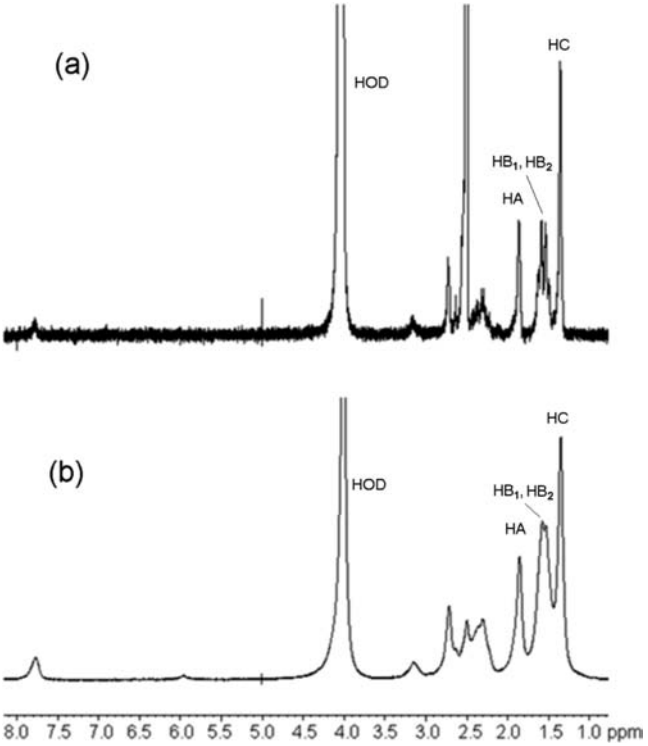

Figure 6. ^{1}H NMR of **3** in d_6-DMSO/D_2O 4:1 (v/v). (a) $[\mathbf{3}]$ = 2 mM, (b) $[\mathbf{3}]$ = 40 mM. The peak at 2.54 ppm is DMSO, while the peak at ~7.8 ppm is the amide NH reso.

dx.doi.org/10.1021/ic400989v | Inorg. Chem. 2013, 52, 9418−9426

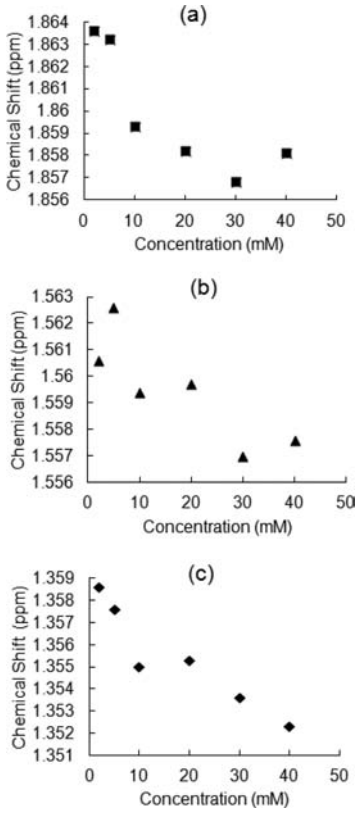

Figure 7. ^{1}H NMR chemical shifts of the protons on the adamantane residue of **3**, (a) H_A, (b) H_B, (c) H_C as a function of the concentration of **3** in d_6-DMSO/D_2O 4:1 (v/v).

$$2\cdot\mathbf{3} \overset{K_2}{\rightleftharpoons} (\mathbf{3})_2 \tag{7}$$

To determine the dimerization constant K_2:

$$K_2 = \frac{[(\mathbf{3})_2]}{[\mathbf{3}]^2} \tag{8}$$

we analyzed the data of Figure 7. Details are given in the Supporting Information. The value found for K_2 was 26.7 M^{-1}.

In principle, the self-association of **3** should be taken into account in the binding model. In addition to eq 6, we should consider the dimerization equilibrium, eq 8.

The chemical shift of one of the three AD protons, if binding and dimerization occur simultaneously, is

$$\delta = f_o\delta_o + f_d\delta_d + f_b\delta_b \tag{9}$$

where f_o, f_d, and f_b are the fractions of **3** in monomeric, dimeric, and CD-bound forms, and δ_o, δ_d, and δ_b are the corresponding chemical shifts. When the concentration of **3** approaches 0, all of **3** is in monomeric form. Of course, $f_o + f_d + f_b = 1$. Equation 6 now is written

$$K = \frac{f_b}{(r - f_b)(16.7\text{ mM})(1 - f_b - f_d)} \tag{10}$$

and eq 8 becomes

$$K_2 = \frac{f_d[\mathbf{3}]_0/2}{\{(1 - f_b - f_d)[\mathbf{3}]_o\}^2} \tag{11}$$

These two equations can be solved to obtain f_d and f_b and subsequently f_o, in terms of K and K_2, so that the chemical shift for each proton can be calculated, given values of δ_o, δ_d, and δ_b. Details are in the Supporting Information.

Although no cyclodextrin was present for the measurements of K_2, the value of K_2 should be the same in the presence of CD. Assuming K_2 = 26.7 M^{-1} and setting δ_o for each proton to the value previously determined, we determined the values of the other seven parameters (K plus δ_b and δ_m for each proton) to minimize the sum of the squared deviations between observed and calculated chemical shifts. The chemical shifts are calculated according to eq 9. The resulting values of the parameters are given in the Supporting Information. In particular, K = 380 M^{-1}, which is essentially the same as the value determined without considering dimerization.

In addition to the above analysis of the binding of **3** to βCD in solution, the actual amount of **3** bound to the cyclodextrin-capped particle, **2**, was determined by mixing **3** with **2**, isolating **4** by centrifugation, and determining the amount of platinum bound using ICP-MS (Experimental Section). For solution concentrations of [**3**] = [βSCD] = 2.58 mM, where [βSCD] is the effective concentration of thiol-cyclodextrin bound to the surface of the nanoparticle, the weight percent of platinum bound to **4** is 2.50%. The average number (n') of **3** loaded onto one AuNP, eq 12, is equal to the number of Pt atoms per nanoparticle, or

$$n' = \frac{\text{wt\%(Pt)}/M''}{\text{wt\%(Au)}/M}N = \frac{\text{wt\%(Pt)}}{M'' \times \text{wt\%(Au)}}\frac{\pi D^3\rho}{6}N_{Av} \tag{12}$$

where M'' is the atomic weight of Pt (195.08 g/mol), M is the atomic weight of gold, N is the number of gold atoms per nanoparticle, D is the nanoparticle diameter, and ρ is the density of gold (19.3 g/cm^3). Inserting these values, this becomes eq 12.

$$n' = 31.20\left(\frac{D}{\text{nm}}\right)^3\frac{\text{wt\%(Pt)}}{\text{wt\%(Au)}} \tag{13}$$

On the basis of the ICP-MS result, wt % (Pt) is 2.50%; with D = 4.7 nm and wt % (Au) = 64.67%, the value of n' is ~125, which means ~60% of the ~210 cyclodextrin sites on AuNP are loaded with complex **3**.

From this result, we can estimate the binding equilibrium constant of **3** to cyclodextrin on the surface of the gold nanoparticle and compare it with the values obtained in the NMR experiments of **3** binding to βCD. Because $[\mathbf{3}]_0$ = $[\beta\text{SCD}]_0$ = 2.58 mM in producing **4**, eq 6 becomes

$$K = \frac{f_b}{(2.58\text{ mM})(1 - f_b)(1 - f_b)} \tag{14}$$

and f_b = 0.595 yields $K = 1.4 \times 10^3$ M^{-1}. This does not take into account the self-association dimerization of **3**, discussed above, but those calculations show that self-association has only a small effect on the value of K (it changed it from 436 to 318 M^{-1}). Because the calculations with the NMR data involve minimizing with respect to seven parameters and only 27 data points, the value $K \approx 1.4 \times 10^3$ M^{-1}, obtained from the loading measurement using ICP-MS, is likely more reliable than the value of K obtained from NMR.

In any case, it is clear that the binding constant from NMR is much smaller than earlier reported adamantane and drug complexes with βCD.[47,48] This reduction in K could be due to the lower dielectric constant of DMSO relative to that of water, the medium in which most values of K for this type of

dx.doi.org/10.1021/ic400989v | Inorg. Chem. 2013, 52, 9418−9426

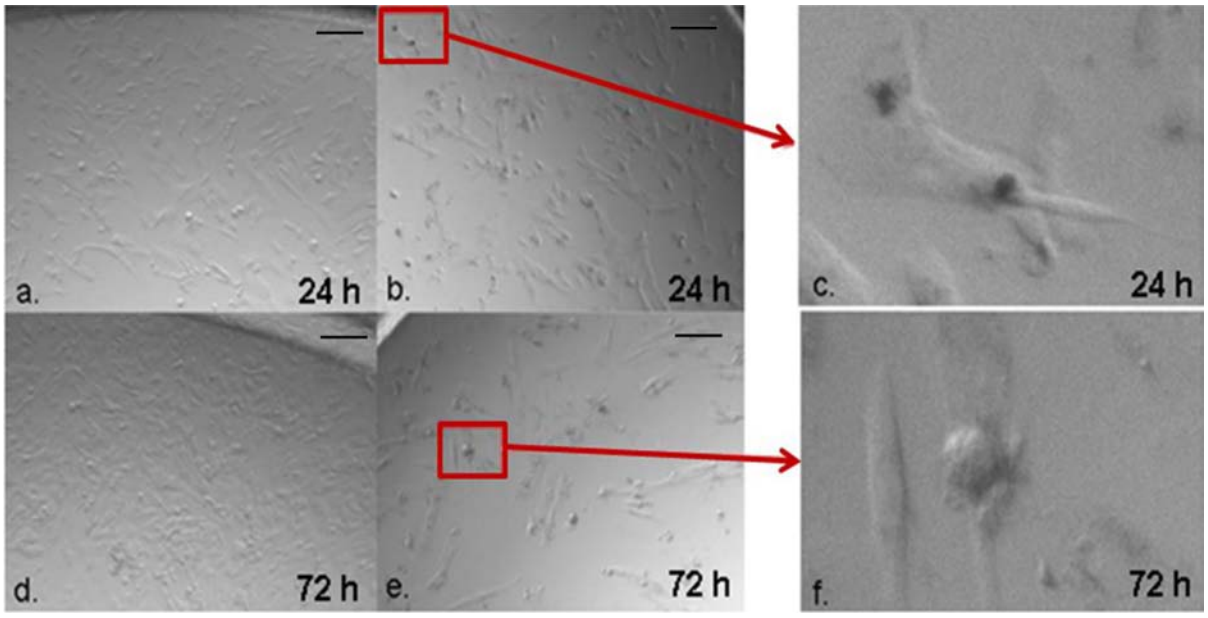

Figure 8. Microscope images of untreated SK-N-SH cells (a and d) and cells treated with **4** (20 μM Pt) for 24 h (b and c) and 72 h (e and f). The dark spots in (b) and (c) are the aggregation of AuNPs in the nucleus of the cell. The scale bar is 100 μm.

interaction have been measured. Preparing **4** in DMSO/water, 4:1, followed by dissolution of the loaded delivery vehicle in culture media or other aqueous solutions would increase the dielectric constant of the medium, thus enhancing the affinity of **3** toward **2**. The discrepancy between the value of K for the **3**−βCD interaction (from NMR) and the corresponding value K for the **2**−**3** interaction (from ICP-MS) could be due to the presence of additional binding sites on the gold nanoparticle **2** that are not present in βCD itself. For example, some fraction of the βSCD units on the surface of the particle are involved in inter- and intramolecular disulfide bonds. Because it is known that a sulfur atom in dimethyldisulfide can react with $[PtMe_3(bpy)(Me_2CO)]BF_4$ by displacement of acetone, it is possible that some of **3** is attached to **2** through a Pt(IV)−sulfur (disulfide) bond leading to the higher value of K observed for the conjugate−nanoparticle interaction.[49]

Because cisplatin and carboplatin are used to treat childhood cancers,[50−52] neuroblastoma SK-N-SH cells were exposed to **4**. Viewing the cells with an optical microscope 24 h after exposure to **4** showed that the gold nanoparticles cluster (individual nanoparticles are too small to be viewed with an optical microscope) in the nuclear regions of cells, Figure 8 (see the Supporting Information for additional images). Interestingly, 72 h after exposure to **4**, when most cells are dying or dead, clusters are no longer observed, showing that nuclear aggregation requires the cell to be alive. While the structural feature of **4** responsible for nuclear clustering is unknown, we earlier reported that fluorescently labeled βCD localizes in the nucleus of SK-N-SH neuroblastoma cells,[36] and Freese et al.[53] showed that gold nanoparticles with surfaced bound amines cluster around the nuclei of primary human dermal microvascular endothelial cells.

Figure 9 shows that treating SK-N-SH cells with **4** for an exposure period of 72 h causes growth inhibition to increase in a dose-dependent manner with a percent inhibition up to ~70% at a Pt concentration of 20 μM. On a per platinum basis, this percent inhibition is less than that of cisplatin, suggesting the Pt(IV) conjugate may not be completely reduced to

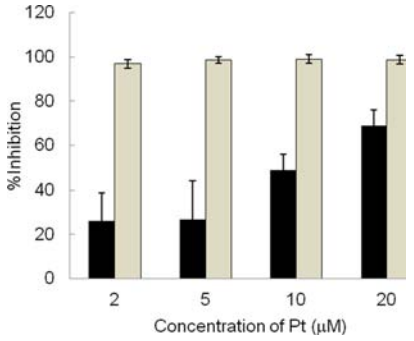

Figure 9. Percent inhibition versus concentration by Pt on **4** (in black) and cisplatin (in gray) after 72 h incubation for different concentrations of **4** and cisplatin.

cytotoxic Pt(II) complexes. Earlier studies by us showed that **3**−βCD and two related Pt(IV) complexes, *c*,*t*,*c*-$[PtCl_2(OH)_2(NH_3)_2]$, oxoplatin, and *c*,*t*,*c*-$[PtCl_2(OH)(O_2CCH_2CH_2CO_2H)(NH_3)_2]$, can be reduced by the bioavailable reducing agents ascorbic acid or glutathione and that the platinum reduction products bind to and unwind closed circular pBR322 DNA.[38,54] When these Pt(IV) complexes are reduced with ascorbic acid, the Pt(II) products produce a DNA unwinding pattern identical to that of cisplatin, indicative of the 1,2 intrastrand cross-link. Clearly, additional work will be needed to determine which cellular components are modified by **4** and the molecular mechanism by which the nanoparticle assembly is able to kill cells.

Despite the enormous effort to develop nanoparticles as delivery vehicles for drugs in cancer chemotherapy, relatively little attention has been paid to the challenges that these agents will face on the road to becoming practical drugs. Dr. Nial J. Wheate,[29] in an insightful editorial recently published in the journal *Nanomedicine*, writes that because these new agents have particle size and drug loading that vary considerably from batch to batch and their synthetic yields are usually low, many nanoparticle-based agents may not be ready for preclinical and

dx.doi.org/10.1021/ic400989v | *Inorg. Chem.* 2013, 52, 9418−9426

clinical trials and ultimately for large-scale manufacture. These shortcomings of nanodrugs were also recently discussed in connection with the nanoparticle assembly having curcumin C3 bound to poly lactic acid-*co*-gylcolic acid.[55]

An additional important challenge for any new nanoparticle-based drug is incorporating it into a stable formulation that can be practically administered to the patient. Many nanosystems are highly "decorated", often containing polyethers that provide long blood circulation times, targeting agents that enhance particle uptake by cells, and toxic entities for killing the cells. While polyfunctionality is the strength of these new nanomedicines, placing multiple copies of different molecules in close proximity on the surface of a small particle greatly increases the likelihood that the different functional groups on the particle will react with each other over time. Because a practical drug formulation must have a reasonably long shelf life, self-reaction that would change the composition of the material would make many polyfunctional nanomaterials now being investigated unsuitable for marketing.[9,29] Instability would be a major concern for polyfunctional nanomaterials containing the platinum drugs, which, because they contain Pt(II), are especially prone to substitution reactions. Although Pt(IV) complexes are much less chemically reactive than their Pt(II) counterparts, they are not substitution inert, suggesting that nano preparations containing Pt(IV) and other potential nucleophiles would lack the long-term stability necessary for creating formulations for clinical use. As we demonstrate in this Article, one way to circumvent the problem of achieving long-term stability of a fully assembled nano formulation is to keep components separate, in this case a Pt(IV) complex and a nano delivery vehicle, and mix the two immediately prior to preclinical/clinical studies. This type of "arming" approach is already in widespread use in nuclear medicine in which a radioisotope, for example, pertechnetate, is reacted with a kit containing ligands and other agents to produce the radio-imaging drug immediately prior to administration to the patient.[7] Hopefully, the results described in this Article will stimulate interest in incorporating modular assembly methods for constituting polyfunctional nanotherapeutics as a means of eliminating the long-term stability requirement of the fully constituted assembly. It would seem that this would be an excellent way to both preserve the polyfunctional nature of the assembly and enhance the likelihood that the agent would gain regulatory approval for use in cancer chemotherapy.

CONCLUSIONS

In this Article, we describe the synthesis and characterization of a unique gold nanoparticle with surface-bound thiolated-β-cyclodextrin, which binds an adamantine-appended Pt(IV) prodrug of cisplatin through a guest−host interaction. Because βCD can bind a wide range of drugs and other small molecules, the gold nanoparticle is useful in a variety of drug delivery applications. NMR and thermal gravimetric analysis showed that some of the thiolated cyclodextrin molecules on the surface of the particle have been oligomerized through disulfide bonds, producing a higher than expected cyclodextrin coverage on the particle. The guest−host interaction between the prodrug and βCD in solution was studied using proton NMR which allowed determination of the dimer association constant of the prodrug as well as the binding constant, K, of the prodrug toward βCD. The latter was comparable to the value of K for binding of the prodrug to cyclodextrin molecules on the surface of the gold nanoparticle determined using ICP-MS. Exposure of SK-N-SH neuroblastoma cells to the drug-loaded vehicle resulted in the uptake and clustering of the nanoparticles in the nuclear region of the live cell. However, when the cell is dying or dead, clustering dissipates and cannot be observed with optical microscopy. The armed delivery vehicle is shown to be cytotoxic to neuroblastoma cells, but less cytotoxic than cisplatin itself, suggesting that the prodrug Pt(IV) complex may not be efficiently reduced to cytotoxic Pt(II) species in the cellular milieu. The described guest−host approach for the rapid modular assembly of a potential nanotherapeutic may be a way to eliminate the need for high stability of a fully constituted polyfunctional nanoassembly in a drug formulation.

ASSOCIATED CONTENT

Supporting Information

Additional information concerning the binding models used and associated equations, ^{1}H and ^{13}C NMR spectra and the mass spectrum of βSCD, **1**, plots of the chemical shifts of the protons of substituted adamantanes as a function of concentration, and microscopic images of cells. This material is available free of charge via the Internet at http://pubs.acs.org.

AUTHOR INFORMATION

Corresponding Author

*Tel.: 315-443-4601. Fax: 315-443-4070. E-mail: jcdabrow@syr.edu.

Notes

The authors declare no competing financial interest.

ACKNOWLEDGMENTS

We thank Professors Y. Luk and M. M. Maye as well as Ms. C. Alexander of the Department of Chemistry, Syracuse University, for helpful discussions. Thanks also to the Syracuse Biomaterials Institute of Syracuse University for the use of cell culture facilities and a microscope/camera system for imaging the cells. We are grateful to the Department of Chemistry for financial support of this research.

REFERENCES

(1) Dreaden, E. C.; Austin, L. A.; Mackey, M. A.; El-Sayed, M. A. *Ther. Delivery* **2012**, *3*, 457−78.
(2) Arvizo, R. R.; Bhattacharyya, S.; Kudgus, R. A.; Giri, K.; Bhattacharya, R.; Mukherjee, P. *Chem. Soc. Rev.* **2012**, *41*, 2943−70.
(3) Llevot, A.; Astruc, D. *Chem. Soc. Rev.* **2012**, *41*, 242−57.
(4) Rana, S.; Bajaj, A.; Mout, R.; Rotello, V. M. *Adv. Drug Delivery Rev.* **2012**, *64*, 200−16.
(5) Craig, G. E.; Brown, S. D.; Lamprou, D. A.; Graham, D.; Wheate, N. J. *Inorg. Chem.* **2012**, *51*, 3490−7.
(6) Vigderman, L.; Zubarev, E. R. *Adv. Drug Delivery Rev.* **2012**, May 18.
(7) Dabrowiak, J. C. *Metals in Medicine*; Wiley: United Kingdom, 2009.
(8) Feng, Lu.; Doane, T. L.; Zhu, J.-J.; Burda, C. *Inorg. Chim. Acta* **2012**, *393*, 142−153.
(9) Kim, D.; Jon, S. *Inorg. Chim. Acta* **2012**, *393*, 154−164.
(10) Alexander, C. M.; Maye, M. M.; Dabrowiak, J. C. *Chem. Commun.* **2011**, *47*, 3418−20.
(11) Alexander, C. M.; Dabrowiak, J. C.; Maye, M. M. *Bioconjugate Chem.* **2102**, *23*, 2061−70.
(12) Libutti, S. K.; Paciotti, G. F.; Byrnes, A. A.; Alexander, H. R., Jr.; Gannon, W. E.; Walker, M.; Seidel, G. D.; Yuldasheva, N.; Tamarkin, L. *Clin. Cancer Res.* **2010**, *16*, 6139−49.
(13) Kelland, L. R., Farrell, N. P., Eds. *Platinum-Based Drugs in Cancer Chemotherapy*; Humana Press: Totowa, NJ, 2000.

(14) Guven, A.; Rusakova, I. A.; Lewis, M. T.; Wilson, L. J. *Biomaterials* **2012**, *33*, 1455−1461.
(15) Comenge, J.; Romero, F. M.; Sotelo, C.; Dominguez, F.; Puntes, V. *J. Controlled Release* **2010**, *148*, e31−2.
(16) Dahr, S.; Daniel, W. L.; Giljohann, D. A.; Mirkin, C. A.; Lippard, S. J. *J. Am. Chem. Soc.* **2009**, *131*, 14652−14653.
(17) Brown, S. D.; Nativo, P.; Smith, J. A.; Stirling, D.; Edwards, P. R.; Venugopal, B.; Flint, D. J.; Plumb, J. A.; Graham, D.; Wheate, N. J. *J. Am. Chem. Soc.* **2010**, *132*, 4678−84.
(18) Lin, C. H.; Cheng, S. H.; Liao, W. N.; Wei, P. R.; Sung, P. J.; Weng, C. F.; Lee, C. H. *Int. J. Pharm.* **2012**, *429*, 138−47.
(19) Tao, Z.; Toms, B.; Goodisman, J.; Asefa, T. *ACS Nano* **2010**, *4*, 789−94.
(20) Tao, Z.; Xie, Y.; Goodisman, J.; Asefa, T. *Langmuir* **2010**, *26*, 8914−24.
(21) Di Pasqua, A. J.; Wallner, S.; Kerwood, D. J.; Dabrowiak, J. C. *Chem. Biodiversity* **2009**, *9*, 1343−49.
(22) Kirkpatrick, G. J.; Plumb, J. A.; Sutcliffe, O. B.; Flint, D. J.; Wheate, N. J. *J. Inorg. Biochem.* **2011**, *105*, 1115−22.
(23) Harper, B. W.; Krause-Heuer, A. M.; Grant, M. P.; Manohar, M.; Garbutcheon-Singh, K. B.; Aldrich-Wright, J. R. *Chem.-Eur. J.* **2010**, *16*, 7064−77.
(24) Haxton, K. J.; Burt, H. M. *J. Pharm. Sci.* **2009**, *98*, 2299−316.
(25) Sanchez-Cano, C.; Hannon, M. J. *Dalton Trans.* **2009**, *28*, 10702−11.
(26) Starhopoulos, G. P.; Boulikas, T. *J. Drug Delivery* **2012**, *2012*, 581363.
(27) Nowotnik, D. P.; Cvitkovic, E. *Adv. Drug Delivery Rev.* **2009**, *61*, 1214−19.
(28) Zhou, D.; Xiao, H.; Meng, F.; Zhou, S.; Guo, J.; Li, X.; Jing, X. *Bioconjugate Chem.* **2012**, *23*, 2335−45.
(29) Wheate, N. J. *Nanomedicine* **2012**, *7*, 1285−87.
(30) Di Pasqua, A. J.; Kerwood, D. J.; Shi, Y.; Goodisman, J.; Dabrowiak, J. C. *Dalton Trans.* **2011**, *40*, 4821−25.
(31) Laza-Knoerr, A. L.; Gref, R.; Couvreur, P. *J. Drug Targeting* **2010**, *18*, 645−56.
(32) Cao, R.; Villalonga, R.; Fragoso, A. *IEE Proc. Nanobiotechnol.* **2005**, *152*, 159−64.
(33) Liu, J.; Mendoza, S.; Roman, E.; Lynn, M. J.; Xu, R.; Kaifer, A. E. *J. Am. Chem. Soc.* **1999**, *121*, 4304−4305.
(34) Park, C.; Youn, H.; Kim, H.; Noh, T.; Kook, Y. H.; Oh, E. T.; Park, H. J.; Kim, C. *J. Mater. Chem.* **2009**, *19*, 2310−15.
(35) Heo, D. N.; Yang, D. H.; Moon, H. J.; Lee, J. B.; Bae, M. S.; Lee, S. C.; Lee, W. J.; Sun, I. C.; Kwon, I. K. *Biomaterials* **2012**, *33*, 856−66.
(36) Prashar, D.; Shi, Y.; Bandyopadhyay, D.; Dabrowiak, J. C.; Luk, Y.-Y. *Bioorg. Med. Chem. Lett.* **2011**, *21*, 7421−25.
(37) Halámiková, A.; Heringová, P.; Kaspárková, J.; Intini, F. P.; Natile, G.; Nemirovski, A.; Gibson, D.; Brabec, V. *J. Inorg. Biochem.* **2008**, *102*, 1077−89.
(38) Shi, Y.; Dabrowiak, J. C. *Inorg. Chim. Acta* **2012**, *393*, 337−339.
(39) Li, X.; Qi, Z.; Liang, K.; Bai, X.; Xu, J.; Liu, J.; Shen, J. *Catal. Lett.* **2008**, *124*, 413−417.
(40) Gadelle, A.; Defaye, J. *Angew. Chem., Int. Ed. Engl.* **1991**, *30*, 78−80.
(41) Rojas, M.; Königer, R.; Stoddart, J. F.; Kaifer, A. E. *J. Am. Chem. Soc.* **1995**, *117*, 336−43.
(42) Jain, P. K.; Lee, K.-S.; El-Sayed, I. H.; El-Sayed, M. A. *J. Phys. Chem. B* **2006**, *110*, 7238−48.
(43) Liu, X.; Atwater, M.; Wang, J.; Huo, Q. *Colloids Surf., B* **2007**, *58*, 3−7.
(44) Martin Del Valle, E. M. *Process Biochem.* **2004**, *39*, 1033−46.
(45) Bass, S. W.; Evans, S. A., Jr. *J. Org. Chem.* **1980**, *45*, 710−15.
(46) Grishina, A.; Stanchev, S.; Kumprecht, L.; Buděšinský, M.; Pojarová, M.; Rumlová, M.; Křížová, I.; Rulíšek, L.; Kraus, T. *Chemistry* **2012**, *18*, 12292−304.
(47) Challa, R.; Ahuja, A.; Ali, J.; Khar, R. K. *AAPS PharmSciTech* **2005**, *6*, E329.
(48) Granadero, D.; Bordello, J.; Pérez-Alvite, M. J.; Novo, M.; Al-Soufi, W. *Int. J. Mol. Sci.* **2010**, *11*, 173−188.
(49) Linder, R.; Wagner, C.; Steinborn, D. *Trans. Met. Chem.* **2010**, *35*, 19−25.
(50) Gaynon, P. S.; Ettinger, L. J.; Baum, E. S.; Siegel, S. E.; Krailo, M. D.; Hammond, G. D. *Cancer* **1990**, *66*, 2465−2469.
(51) Helt-Cameron, J.; Allen, P. J. *Pediatr. Nurs.* **2009**, *35*, 121−127.
(52) Estlin, E. J.; Veal, G. J. *Cancer Treat. Rev.* **2003**, *29*, 253−273.
(53) Freese, C.; Gibson, M. I.; Klok, H.-A.; Unger, R. E.; Kirkpatrick, C. J. *Biomacromolecules* **2012**, *13*, 1533−1543.
(54) Shi, Y.; Liu, S.-A.; Kerwood, D. J.; Goodisman, J.; Dabrowiak, J. C. *J. Inorg. Biochem.* **2011**, *107*, 6−14.
(55) Ranjan, A. P.; Mukerjee, A.; Helson, L.; Vishwanatha, J. K. *J. Nanobiotechnol.* **2012**, *10*, 38.